J Appl Electrochem (2009) 39:1883–1887
DOI 10.1007/s10800-009-9893-3

ORIGINAL PAPER

Using a galvanostatic anodization system as a water heater

M. S. Sikora · F. Trivinho-Strixino · M. E. B. R. Bello · E. C. Pereira

Received: 29 August 2008 / Accepted: 1 April 2009 / Published online: 18 April 2009

Abstract The aim of this paper is to evaluate the application of valve metal anodization to water heating. The solution heating occurs during the oxide breakdown region, a potential oscillation region where the main process is the electronic current associated with the water oxidation reaction over the oxide surface. It was observed that the heating rate is influenced by the current density since the temperature rise is governed by the spark events during the galvanostatic growth. The heating rate of the galvanostatic heater was compared with some commercial heaters, and found to be 14% higher than a commercial resistance-based heater and 29% higher than a shower element.

Keywords Valve metals · Galvanostatic anodization · Zirconium · Water heater

1 Introduction

Valve metals (Nb, Ta, Zr, Ti, Hf, Al) are known to form spontaneously stable oxide layers over their surfaces under ambient conditions [1], making these materials very resistant to corrosion. Besides the corrosion resistance, these metals have been studied in relation to a wide range of applications of their oxides, such as photocatalyst [2–5], biomaterials for medical implants [6, 7], electronic applications [8, 9], solar cells [10] and sensors [11].

The oxides can be prepared by several techniques, including: thermal oxidation [12, 13], sol–gel routes [14], sputtering [15] and anodization [1, 16]. This last procedure has certain advantages: low cost and, especially, the possibility of obtaining self-organized materials such as porous or tubular structures on a nanometric scale [17, 18].

Anodic oxide growth can be performed by either potentiostatic or galvanostatic procedures. The first is normally used in the preparation of self-organized materials such as porous anodic alumina, PAA. In the galvanostatic procedure, the electrode potential is adjusted to maintain a constant current through the electrochemical system. Thus, high electric fields are observed, such as 10^7 V cm^{-1}, depending on the material and the experimental conditions. Generally, the galvanostatic potential versus time curve is characterized by two distinct regions during anodization. Initially, there is an almost linear increase in the potential which is generally attributed to the ionic character of the current in this region. If we suppose that the molar volume and the current efficiency to be constant, the film thickness increases linearly with the potential [1, 19]. The second region is characterized by an oscillatory potential, associated with the dielectric breakdown of the oxide film [19]. In this region, the current is mainly electronic and results from electrons injected into the film from the oxidation of water [19, 20]. It is known that, in the breakdown region, the oxide is locally destroyed and rebuilt throughout the experiment [1]. This dynamic change in the local oxide thickness could be the factor that leads to potential oscillation. As described in the literature [1], experimental conditions such as electrolyte composition, electrolyte concentration, applied current or

M. S. Sikora · M. E. B. R. Bello · E. C. Pereira (✉)
Laboratório Interdisciplinar de Eletroquímica e Cerâmica (LIEC), DQ, UFSCar, Cx.P.:676, Sao Carlos, SP 13565-905, Brazil
e-mail: decp@ufscar.br

F. Trivinho-Strixino
Universidade Federal de São Carlos, Campus Sorocaba, Sorocaba, SP 18052-780, Brazil

potential and solution temperature have an important influence on the properties of the oxide produced.

In any case, during galvanostatic oxide film formation, it is observed that the product of the destruction of the oxide passes into the solution, as soluble material, in an exothermic process; the attainment of thermal equilibrium with the solution thus leads to an increase in its temperature. To avoid this "problem", galvanostatic oxide film formation is usually performed in a thermostatically-controlled electrochemical cell which allows the temperature to be set by a heat exchanger. Here, we proposed a different approach in order to use the heat generated during the valve metal anodization. We investigated the effect of various preparation parameters on the heating rate and, finally, compared these results with those obtained with some commercial heaters, to assess the water-heating efficiency of the anodization process.

2 Experimental procedure

A two-electrode electrochemical cell was used to perform the galvanostatic anodization of zirconium. A zirconium sheet (Alfa Aesar, 99.99%, 0.25 mm thick) with an exposed area of 2 cm^2, and a platinum sheet were used as working and counter electrodes. Prior to the experiments, the working electrode was polished with #600 SiC and then with #1200 SiC emery paper followed by vigorous washing with deionized water.

To investigate the effect of each preparation parameter on the temperature increase rate, we performed a factorial design [21]. Factorial design is a tool which can be used to investigate the effects of various experimental factors on the response variable and has the advantage that it decreases the number of experiments that must be performed to obtain a statistical result from the system and detects interactions between factors. In this method, the number of experiments to be performed is n^k, where "n" is the number of values tested for each experimental factor and "k" is the number of experimental factors. Here, we investigated three different variables at two different levels each: acid composition (H_3PO_4 or $H_2C_2O_4$), acid concentration (0.1 or 0.3 mol L^{-1}) and current density (10 and 20 mA cm^{-2}), as listed in Table 1. Then we performed eight experiments in duplicate to assess the standard deviation of the heating efficiency.

The experiments were carried out under galvanostatic conditions with a home-made current source, measuring the potential difference between working electrode and counter electrode with an HP® 34410A multimeter coupled to a computer by an in-house software routine developed with HP-VEE® 5.0 software. To follow the temperature increase as a function of time, a MINIPA® MT-600 thermocouple was placed inside the electrolyte bath. All measurements were made in 100 mL of electrolyte solution. All electrochemical experiments were carried out inside a calorimeter. The calorimeter was calibrated and its heat capacity was previously determined.

Table 1 2^3 Factorial design used to find the best anodization conditions

Sample	Acid composition	Concentration (mol L^{-1})	Current density (mA cm^{-2})
1	$H_2C_2O_4$	0.1	10
2	H_3PO_4	0.1	10
3	$H_2C_2O_4$	0.3	10
4	H_3PO_4	0.3	10
5	$H_2C_2O_4$	0.1	20
6	H_3PO_4	0.1	20
7	$H_2C_2O_4$	0.3	20
8	H_3PO_4	0.3	20

Finally, a comparative study was carried out among the anodization system, 5.6 Ω commercial shower element and a 70 Ω water heater. To assess the heating efficiency of the anodization process, the average potential within the breakdown region was calculated. The resulting dissipated power (P_D) was near to the nominal power of the commercial elements (14 W). All experiments were limited to 50 °C to avoid equipment damage.

3 Results and discussion

Figure 1a presents a typical anodization curve for ZrO_2 film growth when the cell temperature is maintained constant using thermostatic control. At the beginning of the process the potential increases almost linearly to a maximum value. As mentioned in the Introduction, in this region the main current inside the oxide is ionic [1, 19]. After this region, an oscillating potential regime with average potential almost constant is reached, known as the breakdown potential. The main current in the oscillatory part is the electronic current associated with water oxidation [19]. The electrons injected into the film lead to local oxide destruction and reconstruction, leading to the potential oscillation.

Various models have been proposed to describe the dielectric breakdown which occurs during the galvanostatic growth. Ikonopisov [19] proposed the electron avalanche model, where injection of electrons into the oxide conduction band causes electrolytic breakdown. Some of these electrons are accelerated by the electric field, ejecting other electrons by collision. The precursor electrons of the avalanche process result from the oxidation of ionic impurities,

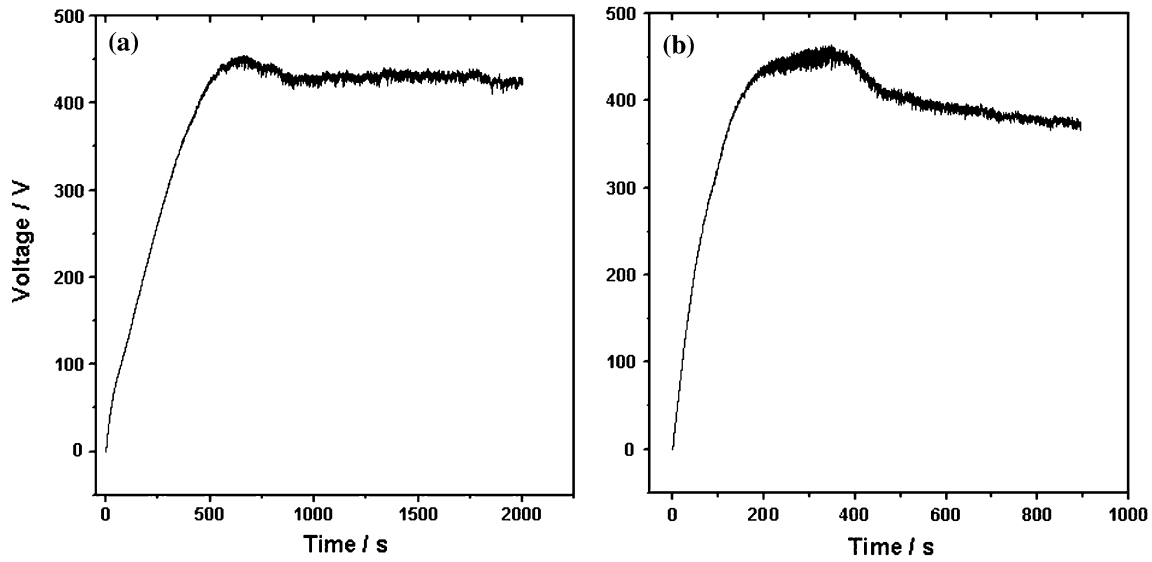

Fig. 1 **a** Anodization curve obtained at 20 mA cm^{-2} and 2 cm^2 of electrode area in 0.1 mol L^{-1} H_3PO_4 under thermostatic control. **b** Anodization curve obtained at 20 mA cm^{-2} and 2 cm^2 of electrode area in 0.1 mol L^{-1} H_3PO_4 without thermostatic control

thus the breakdown is facilitated by presence of these impurities. This phenomenon can be observed as a travelling spark chain or an even burning spark. In addition, Di Quarto et al. [22] proposed that mechanical breakdown precedes the electrolytic breakdown, influencing the oxide growth speed. At present, no model completely describes the electrolytic breakdown that occurs during the anodic growth of valve metals oxides.

Figure 1b depicts the same anodization curve, but with the cell temperature changing freely, without thermostatic control. It can be seen that, after the breakdown potential at around 450 V (after 400 s), there is a potential decrease. Ikonopisov showed that the breakdown potential is inversely proportional to temperature [19]. Hence, this behavior is characteristic of an anodization without temperature control.

In the breakdown region, temperature rise could be explained by the electron avalanche model [19]. In this case, the electrolyte not only supplies ions for the oxidation process, but also promotes the injection of electrons into the conduction band of the oxide, due to water oxidation. These freely-moving electrons are accelerated by the high electric field, and thus acquire enough energy to release other electrons by impact ionization, leading to an avalanche multiplication effect.

In a second set of experiments, the temperature increase in the electrochemical cell was monitored during anodization. The results are presented Fig. 2. In this case, the experimental conditions were varied among the experiments. After 300 s all curves showed a linear increase of temperature as a function of time. To investigate the effect

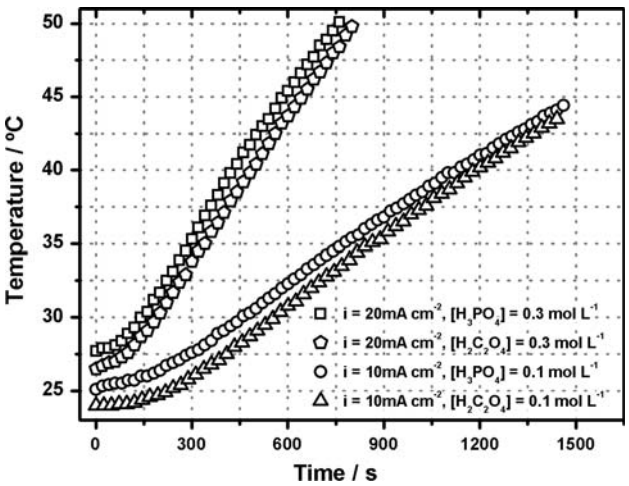

Fig. 2 Temperature rise during galvanostatic anodization

of the preparation variables on the heating efficiency, a factorial experiment was performed using those variables described in Table 1. The system response used was the heater efficiency, calculated as follows:

$$Q_t = Q_1 + Q_2$$

where:

$$Q_1 = m \cdot c \cdot \Delta T$$
$$Q_2 = C_{cal} \cdot \Delta T$$

m = solution mass in the electrochemical cell, c = specific heat capacity of water = 4.18 J K^{-1} g^{-1}, ΔT = temperature variation, C_{cal} = calorimeter heat capacity.

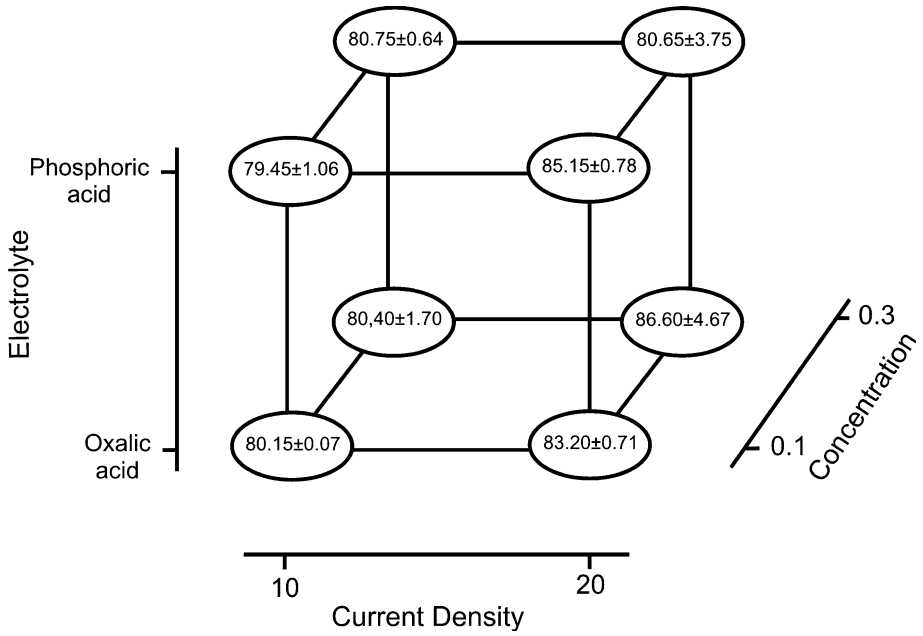

Fig. 3 Geometric representation of the heating efficiency for the galvanostatic anodization of zirconium. Experimental conditions described in Table 1

Table 2 Effects of variables on calculated heat efficiency for those conditions presented in Table 1

Average ± SD	82.04 ± 0.66
Main effects ± SD	
Electrolyte composition	−1.09 ± 1.32
Electrolyte concentration	0.11 ± 1.32
Current density	3.37 ± 1.32
Interaction of two factors ± SD	
12	−1.71 ± 1.32
13	−0.91 ± 1.32
23	−0.66 ± 1.32
Interaction of three factors ± SD	
123	1.21 ± 1.32

The efficiency was calculated as:

$$\text{Efficiency} = \frac{P_G}{P_D} \times 100,$$

where

$$P_G = \frac{Q_t}{\Delta t}$$

$$P_D = V_{RM} \times I$$

V_{RM} = average breakdown potential, I = Applied current.

Here, Q_t represents the total heat produced by the anodization process and water electrolysis, and is composed of the solution heating, Q_1, and the heat spent on heating of the calorimeter Q_2. The efficiency is calculated as the ratio of the generated to the total dissipated power. The dissipated power is the product of the average breakdown potential value, V_{RM}, and the applied current, I, used in the anodization process.

Figure 3 shows the cube representation of the results under all experimental conditions and, at its corners, the heater efficiency calculated for every combination of conditions tested. In this representation, it is clear that the most important factor is the current density. Another important observation that can be extracted from the 2^3 factorial design is the effect of interactions between the factors, i.e., current density, electrolyte composition and electrolyte concentration (Table 2). As can be seen in Table 2, the most important parameter for the heat efficiency is the current density, assuming a Student t-distribution with 8 degrees of freedom. The two other effects alone have no significant effect on the response, considering the experimental error. A possible explanation for this fact is that the rate of temperature increase is governed by the sparking rate during the galvanostatic growth. The electron flux is proportional to current density. Hence, the increase of this variable promotes the enhance of the local oxide destruction rate which accompanies the spark events. In addition, altering the electrolyte composition does not affect the spark events but probably changes the oxide defect density. Finally, changing the electrolyte concentration, would changed the oxide-solution potential drop, but at the concentrations used here no important effect on heater efficiency was seen. Thus, one possible explanation is that the temperature rise is an oxide bulk phenomenon that depends mostly on the spark generation rate.

A comparative study was conducted, involving the anodization system and two types of commercial heater: a shower element and a domestic water heater, of resistance

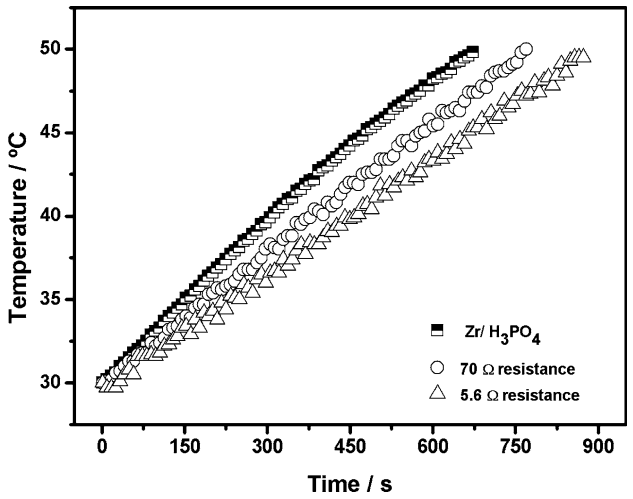

Fig. 4 Comparative study of zirconium anodization system, domestic water heater and shower element, respectively 70 and 5.6 Ω, at a power of 14 W

5.6 and 70 Ω, respectively. In this study, the power dissipated during the experiments was set to 14 W, within the limits of the DC power supply used. Considering the material of the commercial heaters, the acid solution was replaced by deionized water. The results are displayed in Fig. 4. The heating rate for the anodization system is higher than those of the commercial water heater and the shower resistance. The calculated efficiencies were, 71.25 ± 1.48%, 78.8 ± 0.78% and 85.7 ± 2.7%, for the 5.6 Ω, 70 Ω resistances and the anodization system, respectively. It is important to stress that most of the current crossing the oxide is an electronic current produced by water oxidation. Therefore, the metal oxide mass loss is very low in the investigated system. Even in the case of active metal dissolution, which surely does not occur here, the electrode mass used in the present study is sufficient to last up to 345 h of continuous heating. Further investigation will be made to improve the heating rate and to determine the electrochemical stability of the electrodes in a prototype designed specifically for water heating.

4 Conclusion

This study shows that the zirconium anodization system could be used to develop a heating system, as it shows a higher heating rate than other systems used, being at least 14% higher than the commercial water heater and about 29% higher than the shower element. The factorial design revealed that the most important experimental adjustable variable affecting the heater efficiency was the applied current density during anodization. Considering that the current is mainly electronic in the breakdown region, the material dissolution would be very small. Hence, this system could be used for water heating up to 345 h.

Acknowledgements The authors gratefully acknowledge the financial support of the Brazilian research funding agencies FAPESP (proc: 03/09933-8) and CNPq.

References

1. Parkhutik V, Albella JM, Martinez-Duart JM (1992) In: Conway BE et al (eds) Modern aspects of electrochemistry, 1st edn. Plenum Press, New York
2. Wang W, Tao J, Wang T et al (2007) Rare Met 26:136
3. Chenthamarakshan CR, Rajeshwar K (2000) Langmuir 16:2715
4. Tacconi NR, Chenthamarakshan CR, Yogeeswaran G et al (2006) J Phys Chem B 110:25347
5. Watcharenwong A, Chanmanee W, Tacconi NR et al (2008) J Electroanal Chem 612:112
6. Kar A, Raja KS, Misra M (2006) Surf Coat Technol 201:3723
7. Oh S, Jin S (2006) Mat Sci Eng C 26:1301
8. Mozalev A, Surganov A, Magaino S (1999) Electrochim Acta 44:3891
9. Surganov V (1994) IEEE Trans Compon Packag Manuf Technol B 17:197
10. Grätzel M (2001) Nature 414:338
11. Mor GK, Varghese OK, Paulose M et al (2006) Thin Solid Films 496:42
12. Zhang D, Yoshida T, Furuta K et al (2004) J Photochem Photobiol A 164:159
13. Panagopoulos C, Badekas H (1987) Mat Lett 5:307
14. Ge L, Xu M, Sun M et al (2006) J Sol-Gel Sci Technol 38:47
15. Habazaki H, Shimizu K, Nagata S et al (2005) Thin Solid Films 479:144
16. Makushok YE, Parkhutik PV, Martinez-Duart JM et al (1994) J Phys D 27:661
17. Masuda H, Fukuda K (1995) Science 268:1466
18. Wei W, Macak JM, Schmuki P (2008) Electrochem Commun 10:428
19. Ikonopisov S (1977) Electrochim Acta 22:1077
20. Di Quarto F, Piazza S, Sunseri C (1984) J Electrochem Soc 131:2901
21. Bruns RE, Neto BB, Scarminio IS (2002) Como fazer experimentos. UNICAMP, Campinas
22. Di Quarto F, Piazza S, Sunseri C (1986) Corros Sci 26:213